### Title
Cardiotoxicity of the cancer therapeutic agent imatinib mesylate.




### Journal
Nature medicine, 12(8)

### ISSN
1078-8956



### Authors
Kerkelä, Risto
Grazette, Luanda
Yacobi, Rinat
et al.



### Publication Date
2006-08-23

Peer reviewed

nature medicine



# Cardiotoxicity of the cancer therapeutic agent imatinib mesylate

Risto Kerkelä[1,2], Luanda Grazette[3], Rinat Yacobi[4], Cezar Iliescu[5], Richard Patten[2], Cara Beahm[1], Brian Walters[2], Sergei Shevtsov[1,2], Stéphanie Pesant[1], Fred J Clubb[6], Anthony Rosenzweig[3], Robert N Salomon[7], Richard A Van Etten[4], Joseph Alroy[7,8], Jean-Bernard Durand[5] & Thomas Force[1,2]

**Imatinib mesylate (Gleevec) is a small-molecule inhibitor of the fusion protein Bcr-Abl, the causal agent in chronic myelogenous leukemia. Here we report ten individuals who developed severe congestive heart failure while on imatinib and we show that imatinib-treated mice develop left ventricular contractile dysfunction. Transmission electron micrographs from humans and mice treated with imatinib show mitochondrial abnormalities and accumulation of membrane whorls in both vacuoles and the sarco- (endo-) plasmic reticulum, findings suggestive of a toxic myopathy. With imatinib treatment, cardiomyocytes in culture show activation of the endoplasmic reticulum (ER) stress response, collapse of the mitochondrial membrane potential, release of cytochrome *c* into the cytosol, reduction in cellular ATP content and cell death. Retroviral gene transfer of an imatinib-resistant mutant of c-Abl, alleviation of ER stress or inhibition of Jun amino-terminal kinases, which are activated as a consequence of ER stress, largely rescues cardiomyocytes from imatinib-induced death. Thus, cardiotoxicity is an unanticipated side effect of inhibition of c-Abl by imatinib.**

More than 90% of cases of chronic myelogenous leukemia (CML) and about 15% of cases of B-cell acute lymphoblastic leukemia result from the reciprocal translocation t(9;22) in hematopoietic stem cells. This translocation creates the Philadelphia chromosome and the oncogenic fusion protein Bcr-Abl, which incorporates c-Abl, a nonreceptor tyrosine kinase and Bcr, a multidomain protein of uncertain function. Bcr-Abl is constitutively active and localized in the cytosol, where it recruits several signaling pathways, leading to both transformation and activation of cell survival pathways that enhance cell-cycle entry and prevent the normal death of granulocytes[1]. Imatinib mesylate (Gleevec) is a small molecule that potently inhibits the kinase activity of Bcr-Abl and has shown marked effects in individuals with chronic-phase CML (>70% of those treated achieve complete cytogenic remission)[2]. In addition, the drug seems to be well tolerated, and a review on its use does not mention cardiotoxicity[2]. Clinical trials of the agent, however, have reported a relatively high incidence of peripheral edema (63–66%), some of which has been classified as severe (4–5%). In addition, dyspnea has been reported in 12–16% of treated individuals and has been classified as severe in 4–5%[3]. Although these symptoms and signs are difficult to evaluate in individuals with CML, it has become apparent to us in clinical practice that many individuals, including those reported herein, have developed left ventricular dysfunction and even frank congestive heart failure (CHF) without a prior history of heart disease.

Based on these observations, we were concerned that imatinib might be directly toxic or that one of the targets of imatinib (c-Abl, Abl-related gene (Arg; also known as Abl-2), platelet-derived growth factor (PDGF) receptor or c-Kit (the receptor for stem cell factor, SCF)) may have a survival function in cardiomyocytes, similar to Erb-B2, a member of the epidermal growth factor receptor family that is amplified in some breast cancers and is the target of the monoclonal antibody trastuzumab (Herceptin)[1,4–7]. Although Bcr-Abl transduces prosurvival signals in hematopoietic cells, in part by recruitment of the PI3K-Akt, Jak-STAT and Grb2-ERK signaling pathways[1], there is little if any evidence that c-Abl or other known targets of imatinib exert prosurvival effects in cardiomyocytes. Rather, c-Abl has been shown to promote apoptosis of cells exposed to genotoxic stress or oxidant stress[8–11]. That said, there are reports that in some cell types (such as osteoblasts and *Caenorhabditis elegans* germline cells) c-Abl can transduce prosurvival signals in response to genotoxic and oxidant stress[12–15].

Here we report ten individuals who presented with severe CHF without obvious cause while receiving imatinib. We found that imatinib has deleterious effects on cardiomyocytes in culture and

[1]Center for Translational Medicine, Jefferson Medical College, 1025 Walnut Street, Philadelphia, Pennsylvania 19107, USA. [2]The Molecular Cardiology Research Institute, Tufts–New England Medical Center and Tufts University School of Medicine, 750 Washington Street, Boston, Massachusetts 02111, USA. [3]Cardiovascular Research Center, Massachusetts General Hospital and Harvard Medical School, 25 Shattuck Street, Boston, Massachusetts 02115, USA. [4]Molecular Oncology Research Institute, Tufts–New England Medical Center and Tufts University School of Medicine, 750 Washington Street, Boston, Massachusetts 02111, USA. [5]M.D. Anderson Cancer Center and The University of Texas, 1515 Holcombe Boulevard Houston, Texas 77030, USA. [6]Department of Cardiovascular Pathology, Texas Heart Institute, 6770 Bertner Avenue Houston, Texas 77030, USA. [7]Department of Pathology, Tufts–New England Medical Center and Tufts University School of Medicine, 750 Washington Street, Boston, Massachusetts 02111, USA. [8]Tufts Cummings School of Veterinary Medicine, 200 Westboro Road, North Grafton, Massachusetts 01536, USA. Correspondence should be addressed to T.F. (thomas.force@jefferson.edu).

Received 4 May; accepted 14 June; published online 23 July 2006; doi:10.1038/nm1446

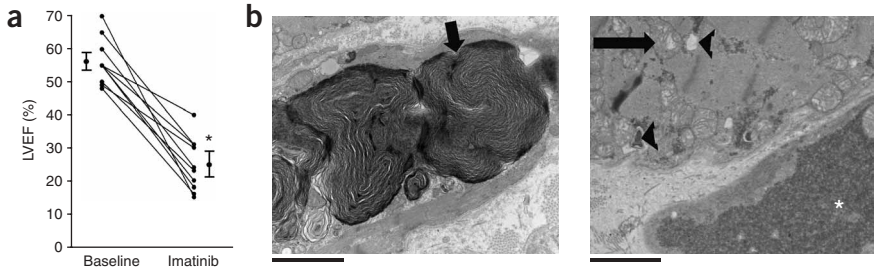


**Figure 1** Imatinib is cardiotoxic in humans. (**a**) Change in left ventricular ejection fraction (LVEF) from pretreatment to presentation with heart failure while on imatinib. The ejection fraction was determined by radionuclide imaging before initiation of imatinib therapy and again at presentation with CHF. $^*P < 0.001$ versus pretreatment value. (**b**) Electron micrographs of cardiac biopsies. Shown are electron micrographs from individuals who presented with presumed imatinib-induced heart failure. Left, arrow indicates a dense membrane whorl. Right, arrow indicates cardiomyocyte mitochondria with partially effaced cristae. Arrowheads indicate dilated sarcoplasmic reticulum with membrane whorls. Asterisk indicates a cardiomyocyte with effaced myofilaments and glycogen accumulation. Scale bars, 2 μm.

*in vivo*. The triggering mechanism seems to be activation of the ER stress response (also known as the unfolded protein response), a response that protects cells by shutting down general protein translation (by PKR-like ER kinase (PERK)-mediated phosphorylation of the translation initiation factor eIF2α) while upregulating the expression of specific protective stress response genes. If ER stress is prolonged, however, prodeath pathways including Jun N-terminal kinases (JNKs) are activated. We show that these pathways are activated in cardiomyocytes exposed to imatinib, leading to profound alterations of mitochondrial function and to cardiomyocyte death.

## RESULTS

### Imatinib cardiotoxicity in humans

We collected clinical data from ten individuals who developed significant left ventricular dysfunction during their course of therapy with imatinib (**Supplementary Table 1** online). All ten individuals had normal left ventricular function before imatinib therapy was instituted (ejection fraction 56 ± 7%), but presented after a mean of 7.2 ± 5.4 months (range 1–14 months) of therapy with heart failure, including significant volume overload and symptoms corresponding to a New York Heart Association (NYHA) class 3–4 heart failure (mean NYHA class 3.5 ± 0.5; $P < 0.001$ versus pretreatment). Ejection fraction by radionuclide imaging at presentation was 25 ± 8% ($P < 0.001$ versus pretreatment ejection fraction; **Fig. 1a**). This low ejection fraction was associated with mild left ventricular dilation (mean left ventricular end-diastolic diameter 57.8 ± 4.8 mm at presentation; range, 52–65 mm; normal range 35–56 mm; ref. 16).

We performed myocardial biopsies on two of these individuals who had no history of coronary artery disease. Transmission electron micrographs of biopsies of the hearts showed prominent membrane whorls in the myocytes (**Fig. 1b**). This abnormality, although nonspecific, has been reported to be characteristic of toxin-induced myopathies[17] and is rarely seen in nonischemic idiopathic dilated cardiomyopathies. Other abnormalities included pleomorphic mitochondria with effaced cristae (**Fig. 1b**), scattered cytosolic lipid droplets and vacuoles (data not shown). In addition, glycogen accumulation in cardiomyocytes was noted (**Fig. 1b**).

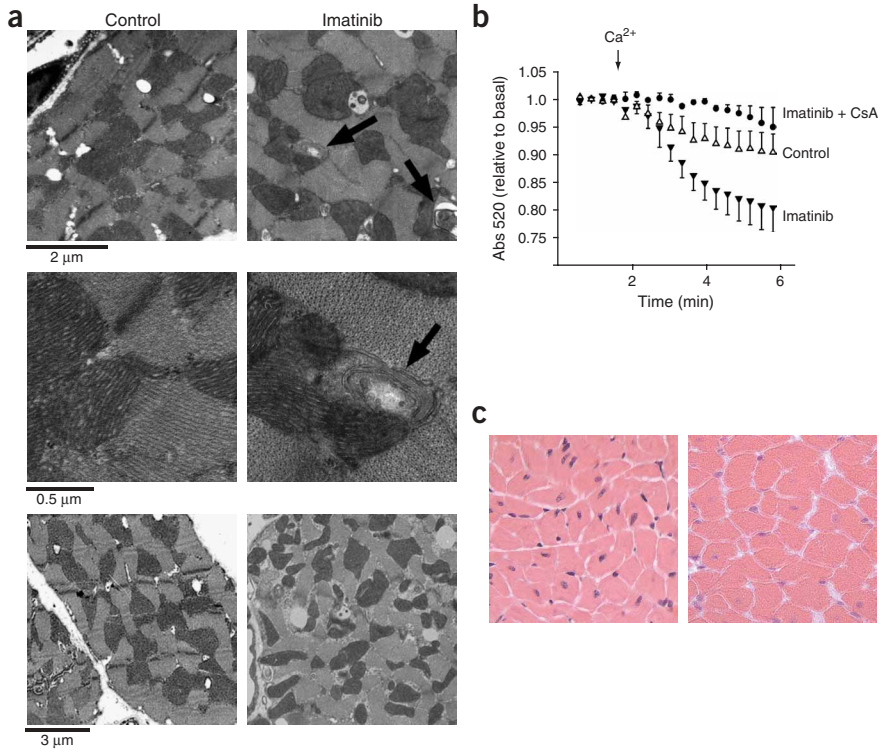


**Figure 2** Imatinib is cardiotoxic in mice. Ultrastructural analysis and assay for mitochondrial permeability transition pore opening. (**a**) Electron micrographs of hearts from mice treated with intraperitoneal injections of vehicle (left ) or imatinib (50 mg/kg/d; right) for 3 weeks. Top panels, sarcoplasmic reticulum and vacuoles containing membrane whorls (arrows). Middle right, a vacuole with a membrane whorl within or immediately adjacent to mitochondria. Bottom right, pleomorphic mitochondria in the imatinib-treated hearts. None of these findings was present in the vehicle-treated hearts. (**b**) Imatinib enhances $Ca^{2+}$-induced mitochondrial swelling. Mitochondria were isolated from hearts of mice treated with either imatinib (200 mg/kg/d) or vehicle for 5 weeks. Swelling, as determined by light scattering, was measured after the addition of 250 μM $Ca^{2+}$. Studies were also done in the presence of cyclosporin A (CsA; 10 mg/ml), an inhibitor of cyclophilin D that blocks opening of the permeability transition pore. (**c**) Hematoxylin and eosin stain of a heart from a mouse treated with either vehicle (left) or imatinib (200 mg/kg/d orally; right) for 5 weeks. Original magnification, ×40.

**Table 1 Echocardiographic indices of imatinib-treated mice**

| | Vehicle | Imatinib 200 mg/kg (5 weeks) |
|---|---|---|
| FS (%) | 28.7 ± 3.63 | 19.9 ± 0.86** |
| EF (%) | 49.0 ± 5.00 | 35.8 ± 1.43** |
| LVEDD (mm) | 3.79 ± 0.19 | 4.17 ± 0.24* |
| LVESD (mm) | 2.76 ± 0.13 | 3.36 ± 0.17*** |
| LVW/BW (mg/g) | 4.68 ± 0.29 | 3.72 ± 0.27** |

FS, fractional shortening; EF, ejection fraction; LVEDD, left ventricular end-diastolic dimension; LVESD, left ventricular end-systolic dimension; LVW/BW, left ventricular mass normalized to body weight ($n = 4$–5). Data are mean ± s.d. *$P < 0.03$ versus vehicle; **$P < 0.003$ versus vehicle; ***$P = 0.0005$ versus vehicle.

## Imatinib cardiotoxicity in mice

To evaluate the possible cardiotoxicity of imatinib, we treated healthy mice with imatinib for 3 or 6 weeks at a dose of 50, 100 or 200 mg/kg/d[18–22]. Transmission electron micrographs of samples from the hearts of three drug-treated mice showed results similar to those seen in studies of individuals on imatinib, including numerous membrane whorls in the sarcoplasmic reticulum, and in or immediately adjacent to mitochondria (**Fig. 2a**). In addition, the sarcoplasmic reticulum was substantially dilated. These findings were not seen in the vehicle-treated controls. As in humans, we noted mitochondrial abnormalities, including evidence of mitochondrial biogenesis—an adaptation typically seen in states of impaired energy generation[23]—with increased numbers of mitochondria (30% increase in mitochondrial number per unit of area; $P < 0.05$ versus vehicle-treated) and pleomorphic mitochondria (**Fig. 2a**). Massons trichrome staining showed no significant fibrosis (data not shown). Studies of mitochondria isolated from the hearts of mice treated with imatinib (200 mg/kg/d) for 5 weeks showed enhanced $Ca^{2+}$-induced opening of the mitochondrial permeability transition pore, as assessed by increased $Ca^{2+}$-induced swelling (**Fig. 2b**). This was largely inhibited by cyclosporin A, an inhibitor of cyclophilin D–mediated pore opening[24]. Thus, imatinib induces ultrastructural abnormalities of mitochondria in humans and in mice, and these are associated with functional abnormalities of mitochondria in mice.

We determined whether we could recapitulate in mice the deterioration in left ventricular function seen in humans on imatinib. Treatment of mice with 200 mg/kg/d, a dose that on the basis of earlier studies was expected to produce blood concentrations comparable to those seen in humans[20–22], led to a significant deterioration in contractile function and moderate left ventricular dilation after 3–4 weeks of treatment (**Table 1**). Thus, in this model, in which

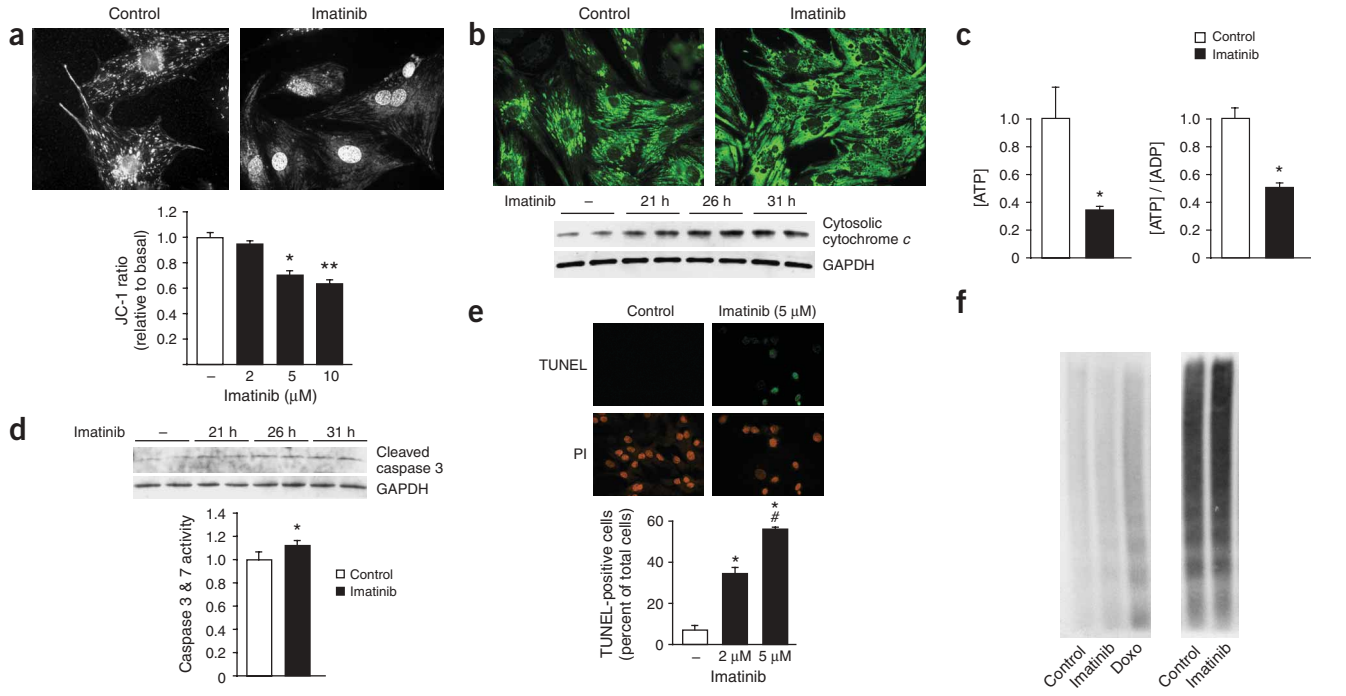


**Figure 3** Effect of imatinib treatment on mitochondrial function and on mediators and markers of apoptosis. (**a**) Imatinib induces loss of mitochondrial membrane potential ($\Delta\psi_m$). NRVMs were treated with vehicle (left) or imatinib (5 μM, right; doses indicated below) for 18 h, and were then loaded with either MitoTracker Red (top) or JC-1 (bottom). MitoTracker Red accumulates in mitochondria in which $\Delta\psi_m$ is maintained and is released into the cytosol when $\Delta\psi_m$ collapses. Punctate (mitochondrial) staining was lacking in the imatinib-treated cells. For JC-1, a decrease in the red/green ratio is a measure of loss of $\Delta\psi_m$. *$P < 0.01$ versus control, **$P < 0.001$ versus control. Original magnification, ×40. (**b**) Imatinib induces cytochrome *c* release. NRVMs were treated with imatinib (5 μM, right) or vehicle (control; left) for 24 h and were fixed and stained for cytochrome *c* (top panels). There was marked release of cytochrome *c* as well as numerous unstained circular structures in the cytosol, compatible with vacuoles (see **Fig. 4a**). Immunoblot confirms release of cytochrome *c* into the cytosol after imatinib treatment for the durations indicated. Original magnification, ×40. (**c**) ATP depletion in NRVMs treated with imatinib (5 μM) for 24 h. Shown are the ATP concentration (left) and the ratio of ATP to ADP (right). Data are normalized to 1.0 for vehicle-treated cells. *$P < 0.05$ versus control. (**d**) Cleavage of caspase 3 and activity of caspases 3 and 7 after treatment of cardiomyocytes with vehicle or imatinib (5 μM) for the time noted (top) or for 26 h (bottom). Data are normalized to 1.0 for vehicle-treated cells. *$P < 0.05$ versus control. (**e**) TUNEL assay. NRVMs were treated with vehicle versus imatinib (5 μM, top; concentrations indicated below) for 24 h before staining with TUNEL. In the graph, TUNEL-positive cells are expressed as a percentage of the number of total cells, as determined by staining postfixation with propidium iodide (PI). *$P < 0.001$ versus control; #$P < 0.05$ versus low-dose imatinib. Original magnification, ×40. (**f**) DNA laddering. NRVMs were treated with vehicle, imatinib (5 μM) or, as a positive control, doxorubicin (1 μg/ml; Doxo) for 24 h before DNA laddering was determined. The amount of DNA used for the reaction was 2 μg (left) or 5 μg (right).

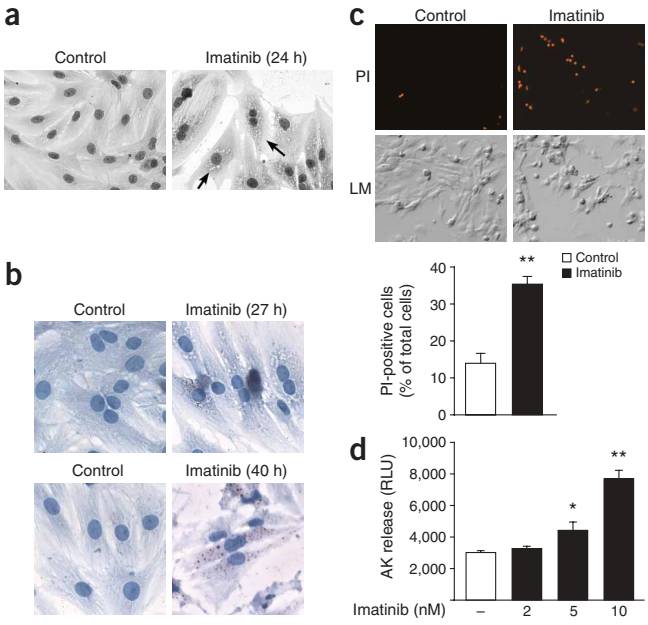


**Figure 4** Effect of imatinib on characteristics of necrotic cell death. (**a**,**b**) Cytosolic vacuolization and lipid droplet accumulation. NRVMs were treated with vehicle or imatinib (5 μM) for the durations shown and were then stained with either hematoxylin and eosin (**a**) or Oil Red-O (**b**) to identify lipid droplet accumulation. There was pronounced cytosolic vacuolization (**a**, arrows) and accumulation of lipid droplets (**b**, red stain). Original magnification, ×40. (**c**) Imatinib induces loss of sarcolemmal integrity as determined by propidium iodide (PI) staining and light microscopy (LM) of live cells. Graph shows the PI-positive cells (those that have lost cell membrane integrity) as a percentage of the total number of cells. Imatinib treatment (5 μM) was carried out for 26 h. $^{**}P < 0.001$ versus control. Original magnification, ×20. (**d**) Imatinib induces cell death in a dose-dependent manner. NRVMs were treated with increasing concentrations of imatinib for 26 h and cellular toxicity was measured by the release of adenylate kinase (AK) into the cell culture medium. $^{*}P < 0.05$ versus control, $^{**}P < 0.001$ versus control.

there are no comorbidities (unlike in humans), administration of imatinib was sufficient by itself to induce cardiotoxicity, culminating in left ventricular contractile dysfunction and dilatation.

There was a significant reduction in left ventricular mass indexed to body weight in the imatinib-treated mice (**Table 1**). Upon staining with hematoxylin and eosin, however, the cardiomyocyte cross-sectional area was not reduced and was slightly (but not significantly) increased in the hearts of imatinib-treated mice (**Fig. 2c**). These findings are consistent with the idea that myocyte loss is the cause of the reduction in left ventricular mass. Because a TdT-mediated dUTP nick end labeling (TUNEL) assay did not suggest that an increase in apoptosis was the cause (data not shown), we used isolated cardiomyocytes to explore further the mechanism of imatinib cardiotoxicity.

## Imatinib induces cell death in isolated cardiomyocytes

We found that imatinib produced dose-dependent collapse of the mitochondrial membrane potential, as determined by staining with the potential-sensitive fluorochromes MitoTracker Red and JC-1 (**Fig. 3a**). Loss of membrane potential was followed by pronounced release of cytochrome *c* into the cytosol (**Fig. 3b**). There was also a marked decline in cellular ATP content and in the ratio of ATP to ADP (**Fig. 3c**). Although there was evidence of classical apoptosis, as assessed by cleavage of caspase 3 (**Fig. 3d**), increased activity of caspases 3 and 7, and TUNEL positivity (**Fig. 3e**), caspase activation was modest and DNA laddering was absent (**Fig. 3f**). In addition, whereas TUNEL positivity was occasionally accompanied by nuclear pyknosis, the dominant finding was pronounced cytosolic vacuolization (**Fig. 4a**), a morphological hallmark of necrotic death. As assessed by Oil Red-O staining, there was an accumulation of lipid droplets in the cytosol and in some vacuoles (**Fig. 4b**), a finding also noted in the human biopsies (data not shown). Finally, there was loss of sarcolemmal integrity, as determined by enhanced uptake of propidium iodide (**Fig. 4c**), another hallmark of necrotic cell death. This finding was confirmed by an assay that quantifies release from the cell of adenylate kinase, a cytosolic protein that is released when membrane integrity is compromised[25] (**Fig. 4d**). The pan-caspase inhibitor Z-VAD-fmk modestly increased the number of cells showing loss of sarcolemmal integrity by propidium iodide staining (data not shown), suggesting that some of these cells might have undergone apoptotic death but were directed toward necrotic death by caspase inhibition combined with progressive ATP depletion[26,27].

## Signaling mechanisms of imatinib cardiotoxicity

We next examined the mechanisms regulating imatinib-induced cardiomyocyte death. Expression of protein kinase Cδ (PKCδ), which regulates cardiomyocyte death under conditions of ischemia and oxidant stress[28,29], has been reported to be regulated by c-Abl after oxidant stress[12]. We found upregulation and cleavage of PKCδ in the hearts of mice and in cardiomyocytes exposed to imatinib (**Supplementary Fig. 1** online). However, inhibition of PKCδ with the selective PKCδ inhibitor peptide δV1-1 (ref. 28), or with either of two nonselective PKC inhibitors (GF 109203X and Gö 6983), did not block release of cytochrome *c* or loss of sarcolemmal integrity in cardiomyocytes in culture (data not shown). Therefore, PKCδ may be involved in imatinib-induced cardiomyocyte toxicity at a late stage after the cell is committed to die (as has been previously proposed[29]), but it is not necessary for imatinib-induced cardiomyocyte death.

We next investigated what the PKCδ-independent pathway mediating death might be. Because of the pronounced accumulation of membranous debris within, and dilation of, the sarcoplasmic and endoplasmic reticulum in the hearts of imatinib-treated humans and mice, we tested whether the ER stress response pathway[30–32] was recruited. We found significant activation by imatinib of the PERK to eIF2α arm of the stress response in the hearts of imatinib-treated mice, as assessed by an increase in phosphorylation of eIF2α (**Fig. 5a**). This arm of the stress response was also activated in cells in culture, but less markedly than *in vivo* (**Fig. 5a**).

Phosphorylation of eIF2α attenuates protein translation in general but leads to increased translation of specific mRNAs, responses that are thought to be cytoprotective[31]. We therefore examined whether the other principal arm of the ER stress response, IRE1, was activated. IRE1 is both a protein kinase and an endoribonuclease[33]. When IRE1 is activated, its endoribonuclease activity excises an intron from the mRNA of the transcription factor XBP-1, resulting in the conversion of a 267-residue transcriptionally inactive protein, XBP-1u (for unspliced), to a transcriptionally active 371-residue protein, XBP-1s (for spliced)[34]. XBP-1s then induces transcription of one or more proteins involved in ER-mediated protein degradation[35]. We found clear-cut activation of the IRE1 arm, as assessed by increased expression of XBP-1s (**Fig. 5b**). Confirming that the protein identified was XBP-1s, treatment with the proteasome inhibitor MG-132 produced

the characteristic reduction in the amount of XBP-1s[34,35] (**Fig. 5b**). Notably, the imatinib-induced increase in XBP-1s was equivalent to that induced by treatment of the cells with the potent ER stressor thapsigargin (**Fig. 5b**).

To determine whether the increase in ER stress induced by imatinib could be the mechanism triggering cardiomyocyte death, we tested the effects of salubrinal, a small-molecule inhibitor of the dephosphorylation of eIF2α that inhibits cell death selectively induced by ER stressors by maintaining inhibition of the translational control point of the ER stress response[31]. Salubrinal increased phosphorylation of eIF2α and rendered cardiomyocytes resistant to imatinib-induced collapse of the mitochondrial



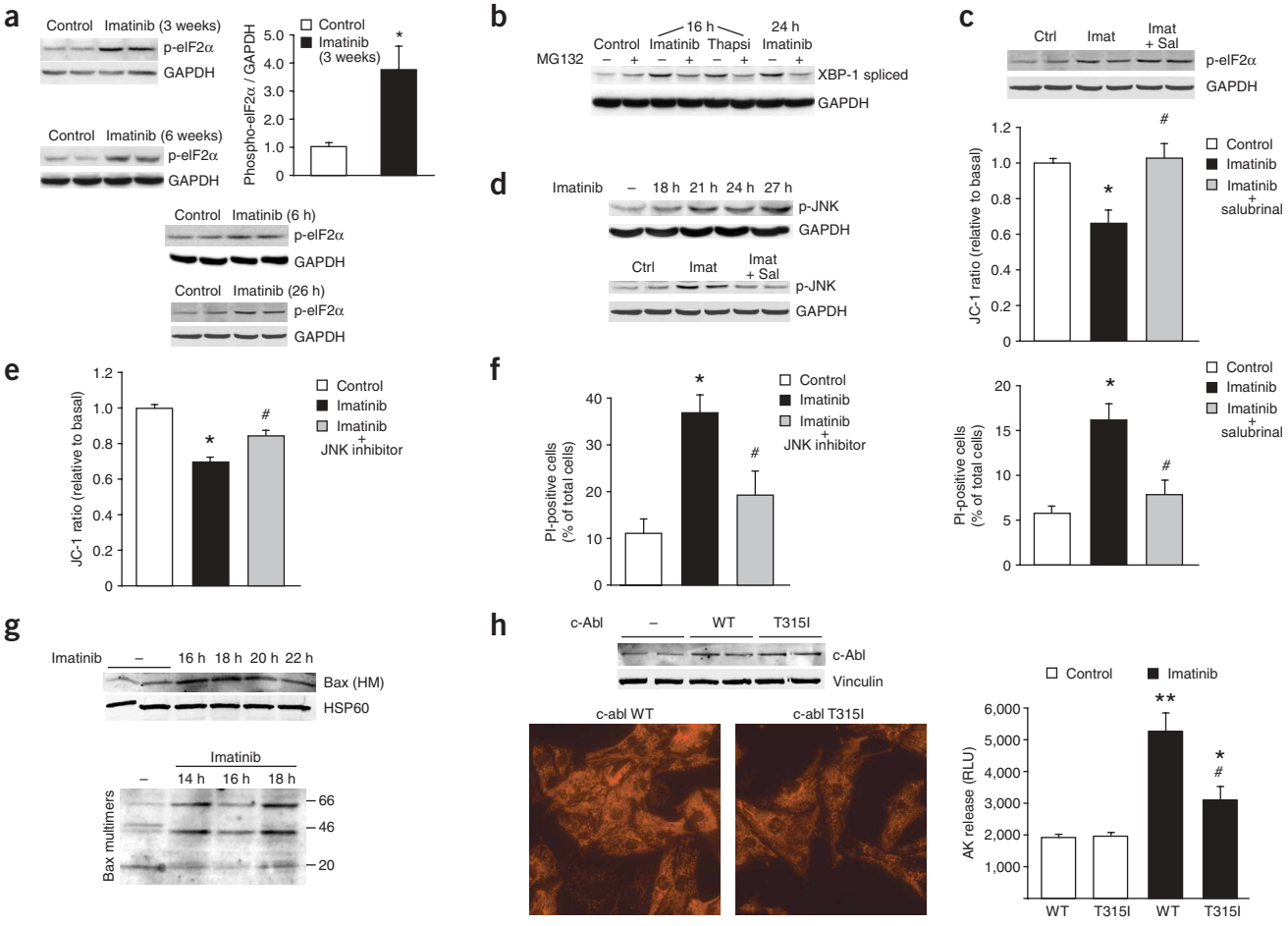


**Figure 5** Signaling pathways regulating imatinib-induced cell death. (**a**) Imatinib activates the ER stress response *in vivo* and *in vitro*. Top left, immunoblot of lysates of hearts from two vehicle-treated and two imatinib-treated mice (50 mg/kg/d for 3 weeks or 100 mg/d for 6 weeks) with a phosphorylation-specific antibody that recognizes activated eIF2α. Top right, phosphorylation of eIF2α *in vivo* normalized to GAPDH as a loading control ($n = 4$). Bottom, phosphorylated eIF2α in lysates of cardiomyocytes in culture treated with imatinib (5 μM) for 6 or 26 h. $^{*}P < 0.05$ versus control. (**b**) Activation of IRE1 by imatinib. Cardiomyocytes were treated with imatinib (5 μM) or thapsigargin (1 μM; Thapsi) with or without the proteasome inhibitor MG-132 (1 μM) for the indicated durations. Cell lysates were then immunoblotted for spliced XBP-1. (**c**) The inhibitor of eIF2α dephosphorylation, salubrinal (Sal), blocks imatinib (Imat)-induced collapse of the mitochondrial potential and cell death. Top, increase in phosphorylated eIF2α in response to treatment with salubrinal. Middle, JC-1 ratio. Bottom, percentage of PI-positive cells. Cells were treated with imatinib (5 μM) or vehicle for either 26 h (top and bottom) or 24 h (middle). Salubrinal (20 μM) was added 6 h after starting the imatinib treatment. Cells were then collected for imunoblotting (top) or for staining with JC-1 (middle) or PI (bottom). In **c** and **f**, PI-positive cells are expressed as a percentage of the number of total cells. $^{*}P < 0.001$ versus control, $^{\#}P < 0.001$ versus imatinib. (**d**) Activation of JNK pathway by imatinib. Top, NRVMs were treated with imatinib (5 μM) for the durations indicated and then lysates were immunoblotted for phosphorylated JNK. Bottom, cells were treated with imatinib (5 μM) for 26 h. Salubrinal (Sal, 20 μM) was added into the cell culture medium 6 h after imatinib. (**e**,**f**) Inhibition of JNK activity protects NRVMs from imatinib-induced collapse of mitochondrial potential and necrotic death. Cells were pretreated with the cell-permeant JNK peptide inhibitor for 1 h, and were then exposed to vehicle or imatinib for 24 h (**e**) or 26 h (**f**) before staining with JC-1 (**e**) or PI (**f**). In **e**, $^{*}P < 0.001$ versus control, $^{\#}P < 0.001$ versus imatinib. In **f**, $^{*}P < 0.001$ versus control, $^{\#}P < 0.01$ versus imatinib. (**g**) Imatinib induces Bax translocation to, and multimerization at, mitochondria. Imatinib- or vehicle-treated NRVMs were subjected to subcellular fractionation to separate the mitochondria-rich heavy membrane fraction (HM). Top, immunoblot showing Bax translocation to mitochondria after treatment with imatinib for the indicated durations. Bottom, immunoblot showing crosslinked BAX multimers. (**h**) Imatinib-induced cytochrome *c* release and cardiomyocyte death are mediated by inhibition of c-Abl. Top left, immunoblot with antibody to c-Abl of lysates from control cells (−) or from cells transduced with either wild-type c-Abl (WT) or c-Abl(T315I). Bottom left, NRVMs transduced with wild-type c-Abl or c-Abl(T315I) were treated with imatinib or vehicle (control) for 24 h, and then fixed and stained for cytochrome *c*. Right, NRVMs transduced with wild-type c-Abl or c-Abl(T315I) were treated with imatinib or vehicle (control) for 26 h, and cellular toxicity was measured by release of adenylate kinase (AK) into the medium. $^{**}P < 0.001$ versus vehicle, $^{*}P < 0.05$ versus vehicle, $^{\#}P < 0.02$ versus wild-type c-Abl plus imatinib. Original magnification, ×40.

membrane potential, as determined by JC-1 (**Fig. 5c**), and cell death, as assessed by propidium iodide staining (**Fig. 5c**). These data are consistent with the idea that the ER stress response is a crucial component of imatinib-induced cell death.

We investigated how the ER stress response might be inducing cardiomyocyte death. As noted above, IRE1-induced expression of XBP-1s is thought to be protective. If the inducing stress is not relieved, however, IRE1 can also signal cell death by activation of the JNK pathway, culminating in mitochondria-dependent cell death[30,36,37]. We therefore examined JNK activation and found marked activation of JNKs both in cultured cardiomyocytes (**Fig. 5d**) and in the hearts of imatinib-treated mice (**Supplementary Fig. 2** online). Salubrinal reduced imatinib-induced JNK activation (**Fig. 5d**), suggesting that ER stress was largely responsible for JNK activation. Treatment of cells with a selective inhibitor of JNK activity, the JNK inhibitor peptide[38], significantly reduced imatinib-induced collapse of the mitochondrial membrane potential, as assessed by JC-1 staining (**Fig. 5e**). In addition, JNK inhibition significantly reduced imatinib-induced cell death, as determined by prevention of the loss of sarcolemmal integrity (**Fig. 5f**). These data support the notion that JNKs have a key role in an imatinib-induced process that culminates in collapse of the mitochondrial membrane potential and necrotic cardiomyocyte death. Inhibition of JNKs had no effect on triggering of the ER stress response by imatinib, as determined by eIF2α phosphorylation, consistent with the idea that JNK activation is downstream of the ER stress response (**Supplementary Fig. 3** online).

JNKs have a host of targets, including Bad, Bax, Bcl2, Bid, Bim, Bmf, c-Jun and FasL (reviewed in ref. 39), any of which could mediate collapse of mitochondrial membrane potential and release of cytochrome *c*. For several of these targets, however, activation of Bax represents a final common pathway. We found evidence of Bax activation, as assessed by translocation of Bax to the mitochondrial fraction and by di- or multimerization of Bax in the mitochondrial fraction of imatinib-treated cardiomyocytes (**Fig. 5g**). Although this translocation was transient, it occurred at a time before cytochrome *c* release and was therefore consistent with imatinib-inducing JNK-dependent cell death through Bax recruitment.

### Imatinib cardiotoxicity is mediated by c-Abl inhibition

We then investigated whether imatinib-induced death was due to inhibition of c-Abl, ARG, the PDGF receptor or an unknown target of imatinib, or to a direct toxic effect of the drug unrelated to kinase inhibition, by comparing the effect of retrovirus-mediated gene transfer of wild-type c-Abl versus an imatinib-resistant mutant of c-Abl, c-Abl(T315I)[40]. More than 90% of cardiomyocytes were successfully transduced, as determined by immunostaining to detect coexpressed green fluorescent protein (data not shown). Retroviral transduction led to expression of the protein that was comparable to endogenous expression (**Fig. 5h**), thereby avoiding the confounding issue of marked overexpression that is seen with adenoviruses.

Gene transfer of c-Abl(T315I) largely inhibited imatinib-induced release of cytochrome *c* (**Fig. 5h**) and protected cells from imatinib-induced cell death, as determined by a cell-death assay (**Fig. 5h**). These findings suggest that imatinib-induced inhibition of c-Abl is essential for the observed cardiomyocyte toxicity and that c-Abl has a previously unknown survival function in cardiomyocytes.

## DISCUSSION

We have shown here that imatinib is cardiotoxic. Several findings, including those from studies of mitochondrial function *ex vivo* (showing enhanced susceptibility to $Ca^{2+}$-induced opening of the mitochondrial permeability transition pore) and from studies in cultured cardiomyocytes (showing collapse of the mitochondrial membrane potential, a marked reduction in ATP concentration, and release of cytochrome *c* in the absence of any other inciting stimulus), identify mitochondria as a chief target of imatinib and implicate mitochondrial dysfunction and the consequent energy rundown as a crucial factor in the cardiotoxicity. Supporting this, electron micrographs of both cardiac biopsies from individuals with imatinib-induced heart failure and the hearts of mice treated with imatinib show mitochondrial abnormalities including pleomorphic mitochondria with effaced cristae.

The effects on cellular energetics were profound, as the ATP concentration dropped by ~65% in the cardiomyocytes. In comparison, treatment of cardiomyocytes with another cardiotoxic chemotherapeutic agent, Herceptin, produces only a 35% decline in ATP[5]. Although a 65% reduction in ATP concentration within an individual cell would probably not compromise many cellular processes, an overall reduction of 65% probably reflects a situation in which there are cells with severe depletion of ATP and others with normal or near-normal levels. Thus, the decline in ATP concentration observed might have significant deleterious consequences on various cellular processes in individual cells. In addition, this energy run-down may largely explain why it was difficult to classify the type of cell death induced by imatinib in cultured cardiomyocytes, which included features of both apoptotic and necrotic cell death. On one hand, there were significant increases in TUNEL-positive cells, but activation of caspases was limited, DNA laddering was not significantly increased and nuclear condensation was not evident at times when injury to the cells was advanced. On the other hand, we observed pronounced cytoplasmic vacuolization and loss of plasma membrane integrity, which are both more characteristic of necrotic death[26]. Because apoptosis is an energy-requiring process, it is possible that the energy rundown induced by imatinib prevented the apoptotic program from being carried out despite the marked release of cytochrome *c*, which should have, in energy-replete cells, triggered the intrinsic pathway[26,27].

Imatinib did not induce release of cytochrome *c* in cardiac fibroblasts, either in cultured primary fibroblasts isolated from neonatal rat heart and passaged in cell culture or in the occasional fibroblast that contaminated the cardiomyocyte cultures (data not shown). The difference in response between cell types may reflect either the well-known differences in the effects of c-Abl (and its inhibition) in distinct types of cells[8–15], or the significantly greater dependence on oxidative phosphorylation for generation of ATP and/or the significantly greater ATP consumption of cardiomyocytes contracting in cell culture.

Although alterations in mitochondrial function seem to be the ultimate cause of imatinib-induced toxicity, our data suggest that activation of the ER stress response, acting through JNKs, occurs upstream of the mitochondrial defects. Imatinib strongly recruited the ER stress response because phosphorylation of eIF2α (a marker of PERK activation) and splicing of XBP-1 (a marker of IRE1 activation) were significantly increased in the hearts of treated mice and in cardiomyocytes in culture[30–33]. Imatinib also triggers ER stress in CML cells expressing Bcr-Abl[41]. Although this observation, like our data, supports the concept that Abl can protect against ER stress, this is not a universal phenomenon, as c-Abl-deficient mouse embryo fibroblasts are protected against ER stress[42]. This difference probably reflects either a 'dosage' effect (partial inhibition with imatinib versus complete deletion) or the different function of c-Abl in different cells,

as noted above[8–15]. The ER stress response is, at least in the initial stages, cytoprotective, because cells with a deletion of eIF2α are more susceptible to ER stress, and overexpression of eIF2α or prevention of eIF2α dephosphorylation with salubrinal are protective[26,27,30,31]. If the inciting stressor is not removed and ER stress is prolonged, however, activation of cell-death pathways ensues[30].

Mediators of cell death originating in the ER are activation and release of caspase 12 (although the relevance of this pathway in humans has been questioned[43]), and IRE1-mediated JNK activation[30]. We saw no cleavage of caspase 12 and no evidence of release of caspase 12 from the ER either *in vivo* or in cultured cells (data not shown). Rather, our data suggest that activation of the JNK pathway is largely responsible for imatinib-induced cardiomyocyte toxicity because treatment of cells with the JNK inhibitor peptide rescued cardiomyocytes from both collapse of the mitochondrial membrane potential and loss of cell membrane integrity. The JNK inhibitor did not alter the imatinib-induced ER stress response, whereas salubrinal decreased imatinib-induced JNK activation, further suggesting that JNKs act downstream of the ER stress response to induce cell death.

JNKs interact with the intrinsic cell death pathway at several points and have been shown to be both sufficient and necessary for release of cytochrome *c* from mitochondria in response to various stimuli[39,44–46]. JNK phosphorylation of 14–3-3 proteins has been shown to release Bax, facilitating its translocation to mitochondria, where it leads to the release of cytochrome *c* (ref. 46). The translocation of Bax to, and oligomerization at, the mitochondrial membrane provides a plausible mechanism by which JNKs lead to collapse of the mitochondrial membrane potential and cell death[39]. However, the marked protective effect of JNK inhibition on loss of sarcolemmal integrity, which was even more pronounced than the protection against loss of mitochondrial membrane potential, raises the possibility of additional effects of JNKs on the necrotic cell death process.

We also examined the effects of imatinib on the activity of various other pro- and antiapoptotic pathways (data not shown). There were minor alterations in the activity of the JAK-STAT and the ERK-RSK signaling pathways, but the magnitude of the changes was small. Other signaling pathways implicated in regulating cell death (for example, Akt and p38-MAPK) were not dysregulated. Although imatinib can lead to release of the serine protease Omi (also known as Htra2) and a necrotic form of cell death in Bcr-Abl–positive cells[47], we did not see significant release of Omi in cardiomyocytes.

The ultrastructural changes, mitochondrial abnormalities and recruitment of the ER stress response were seen with relatively low doses of imatinib (50 mg/kg/d) that are substantially smaller than those used by others (50 mg per kg every morning and 100 mg/kg every evening, or 200 mg/d)[20,22] in mouse models of CML. Although contractile dysfunction was not apparent at this dose, when we used a higher, more relevant dose (200 mg/d), however, mice developed significant contractile dysfunction within 4 weeks.

In conclusion, our data, derived from studies in cultured cardiomyocytes, mice and humans, suggest that imatinib is cardiotoxic and, in humans, can lead to severe left ventricular dysfunction and heart failure. On the basis of our findings, we suggest that a thorough examination of the issue of imatinib-induced left ventricular dysfunction should be undertaken to define the magnitude of the risk. In addition, we suggest that individuals who are on imatinib should be followed closely for symptoms and/or signs of left ventricular dysfunction. Our findings also raise concerns that agents currently in development that target Abl and other nonreceptor tyrosine kinases might be cardiotoxic, and support the importance of prospectively assessing left ventricular function in phase 1–2 and/or phase 3 clinical trials of new agents.

## METHODS

**Materials.** Imatinib mesylate (Gleevec, Novartis) capsules were obtained from Tufts–New England Medical Center pharmacy. The 100-mg capsules were dissolved in distilled water and nonsoluble material was removed by repeated centrifugation at 2,500*g* to yield highly purified material[18]. Antibodies to caspase-12, Bax, PKCδ and cytochrome *c* were from BD Biosciences. Antibody to Omi was from Biovision. Antibodies to cleaved caspase 3 and phosphorylated eIF2α were from Cell Signaling Technology. The general caspase inhibitor Z-VAD-fmk and antibody to glyceraldehyde-3-phosphate dehydrogenase (GAPDH) were from R&D Systems, and antibody to vinculin was from Sigma. Antibody specific for phosphorylated JNK was from Promega. Antibody to HSP-60 was from Stressgen Bioreagents. The Bax-inhibiting peptide, GF 109203x, Gö 6983, JNK inhibitor peptide and salubrinal were from Calbiochem. The PKCδ-inhibiting peptide (δV1-1) was from Kai Pharmaceuticals.

**Subjects.** This research study was approved by the M.D. Anderson Cancer Center Institutional Review Board. The subjects recruited to the study provided informed consent.

**Echocardiography.** The technique used to acquire and analyze echocardiographic data in individuals has been described[48]. The mice were imaged under light sedation (1–1.5% isoflurane) and the data were analyzed as described[49].

**Mice.** We treated age-matched wild-type C57BL6 mice with imatinib mesylate (50, 100 or 200 mg/kg/d) or vehicle for 3 or 6 weeks. The protocol was approved by the Institutional Animal Care and Use Committee at Tufts–New England Medical Center and Thomas Jefferson University.

**Mitochondrial swelling assay.** We homogenized mouse hearts in lysis buffer consisting of 10 mM Tris (pH 7.4), 250 mM sucrose, 1 mM EDTA and protease inhibitors. We centrifuged the homogenate for 5 min at 1,000*g*, removed the supernatant and further centrifuged for 15 min at 10,000*g* to pellet the mitochondria. We washed the pellet twice with buffer consisting of 10 mM Tris (pH 7.4) and 250 mM sucrose, and resuspended the pellet in buffer consisting of 10 mM Tris (pH 7.4), 120 mM KCl and 5 mM $KH_2PO_4$. After 2 h of incubation on ice, we loaded equal amounts of protein into cuvettes and incubated them at 22 °C for 5 min in the presence of 5 mM sodium succinate and 2 μM rotenone. We determined the mitochondrial pore opening by measuring the mitochondrial swelling induced by $CaCl_2$ (250 μM) by detecting light scattering at 520 nm.

**Generation of retroviruses.** We cloned both wild-type and T315I mutant c-ABL Ib[40], in which Thr315 is mutated to isoleucine, into a retroviral expression vector, MIGR1, containing a reporter gene encoding enhanced green fluorescent protein (eGFP). We sequenced the final products to verify the presence or absence of the Thr315→Ile mutation. We cotransfected 293T cells with retroviral vector and the amphotrophic single-genome packaging construct pKat2ampac to produce replication-defective amphotrophic viral stocks. We determined viral titers by transduction of Rat-1 cells, followed by flow cytometric detection of GFP. We transduced neonatal rat ventricular myocytes (NRVMs) with the viruses for 4 h immediately after their isolation, and the experiments were done 2 d after transduction.

**Analysis of mitochondrial membrane potential.** We incubated imatinib-treated myocytes at 37 °C in suspension with F-10 media containing 10 μg/ml JC-1 (Molecular Probes) for 10 min, washed them twice with culture media to remove unbound dye, and subsequently subjected them to fluorescence microscopy. Mitochondria in which the mitocondrial membrane potential is maintained accumulate so-called J-aggregates that fluoresce red, whereas those with a collapsed membrane potential fluoresce green. We calculated the mitochondrial membrane potential for single cells by dividing the intensity of the 590 nm (red) image with its corresponding 525 nm (green) image. We incubated MitoTracker Red (chloromethyl-X-rosamine, 200 nM)

with cells for 10 min. We then washed, fixed and analyzed the cells by fluorescence microscopy.

**Assays for ATP and ADP, and cell viability.** Determination of ATP and the ADP/ATP ratio was done according to manufacturers' instructions (Molecular Probes and Bio-Vision, respectively). For propidium iodide staining, we added medium containing propidium iodide (0.5 μg/ml) for 5 min and visualized the cells immediately by fluorescence and light microscopy. Release of adenylate kinase was measured in culture supernatants by a bioluminescent ToxiLight kit (Cambrex) according to the manufacturer's instructions.

**Histochemical analysis and TUNEL staining.** We plated NRVMs on laminin-coated glass coverslips (40,000 cells/cm$^2$). We fixed cells with 4% paraformaldehyde, blocked them in PBS containing 2% BSA and 0.2% horse serum, and stained them with cytochrome *c*–specific antibody at a dilution of 1:400. Subsequently, we washed the cells twice and added a FITC-conjugated mouse-specific antibody at a dilution of 1:400. For visualization of apoptotic cells by TUNEL assay, we used a kit from MLB International. For Oil Red-O staining, we incubated formalin-fixed coverslips with stain for 10 min, washed them five times with isopropyl alcohol and for 10 min with water, and then counter-stained them with hematoxylin before mounting them.

**Ultrastructural analysis.** We fixed the specimens in Trump fixative (4% formaldehyde and 1% glutaraldehyde in phosphate buffer, pH 7.2) transferred into cacodylate buffer, postfixed them in 1% osmium tetroxide in cacodylate buffer for 3 h at 20 °C, and stained them *en bloc* with 5% aqueous uranyl acetate. We further dehydrated the samples in a graded ethanol series and embedded them in Epon-812. We stained thick sections (1 μm) with toluidine blue. We cut thin sections at 50–70 nm, stained them with uranyl acetate and lead citrate, and photographed them with a Philips EM 201 transmission electron microscope.

**DNA laddering assay.** Cells were collected and DNA was extracted using a kit from Roche. We incubated 2 μg of DNA in 10 μl of buffer consisting of 50 mM Tris (pH 7.5), 10 mM $MgCl_2$, 1 mM dithiothreitol, 50 μg/ml BSA, 10 units of Klenow enzyme and 0.5 μCi of [α-$^{32}$P]dCTP for 10 min at 22 °C. The reaction was stopped by adding 2 μl of gel loading buffer and the samples were then loaded onto a 1.8% agarose gel.

**Statistical analysis.** Differences between data groups were evaluated for significance using Student *t*-test of unpaired data or one-way analysis of variance and Bonferroni post-test. Repeated measures analysis of variance was used for multivariate analysis. All experiments were repeated at least three times and the data are presented as the mean ± s.e.m. unless noted otherwise.

**Other methods.** Cell culture methods, mitochondrial fractionation and immunoblotting are described in **Supplementary Methods** online.

*Note: Supplementary information is available on the Nature Medicine website.*

ACKNOWLEDGMENTS

We thank J. Molkentin, C. Baines and M. Venkatachalam for advice. This work was supported by a grant from the National Heart Lung and Blood Institute (HL67371 to T.F.) and a Specialized Center of Research grant from the Leukemia and Lymphoma Society (to R.A.V.) and grants from the Finnish Heart Foundation and the Paavo Nurmi Foundation (to R.K.).

AUTHOR CONTRIBUTIONS

R.K. performed cell-culture studies, animal studies, generated figures, and helped design the study and write the manuscript. L.G. performed ATP and ADP assays, caspase 3/7 activity assays, Bax translocation and multimerization studies. R.Y. generated retroviruses. C.I. collected patient data. R.P. assisted with performance and analysis of echocardiographic studies. C.B., B.W. and S.S. assisted with cell-culture studies. S.P. assisted with histological studies. F.J.C. analyzed electron micrographs of patient biopsies. A.R. provided expertise for apoptosis studies. R.N.S. provided expertise for histological studies. R.A.V. generated retroviruses, provided expertise on c-Abl, and helped write and edit the manuscript. J.A. analyzed electron micrographs of mouse hearts. J.-B.D. enrolled participants, analyzed patient data and contributed to study design. T.F. (principal investigator) designed studies, interpretated and analyzed data, and drafted and edited the manuscript.

COMPETING INTERESTS STATEMENT

The authors declare that they have no competing financial interests.

Published online at http://www.nature.com/naturemedicine/
Reprints and permissions information is available online at http://npg.nature.com/reprintsandpermissions/

1. Van Etten, R.A. Mechanisms of transformation by the BCR-ABL oncogene: new perspectives in the post-imatinib era. *Leuk. Res.* **28** (Suppl. 1), S21–S28 (2004).
2. Deininger, M., Buchdunger, E. & Druker, B.J. The development of imatinib as a therapeutic agent for chronic myeloid leukemia. *Blood* **105**, 2640–2653 (2005).
3. Cohen, M.H. *et al.* Approval summary for imatinib mesylate capsules in the treatment of chronic myelogenous leukemia. *Clin. Cancer Res.* **8**, 935–942 (2002).
4. Sawyer, D.B., Zuppinger, C., Miller, T.A., Eppenberger, H.M. & Suter, T.M. Modulation of anthracycline-induced myofibrillar disarray in rat ventricular myocytes by neuregulin-1β and anti-erbB2: potential mechanism for trastuzumab-induced cardiotoxicity. *Circulation* **105**, 1551–1554 (2002).
5. Grazette, L.P. *et al.* Inhibition of ErbB2 causes mitochondrial dysfunction in cardiomyocytes: implications for herceptin-induced cardiomyopathy. *J. Am. Coll. Cardiol.* **44**, 2231–2238 (2004).
6. Romond, E.H. *et al.* Trastuzumab plus adjuvant chemotherapy for operable HER2-positive breast cancer. *N. Engl. J. Med.* **353**, 1673–1684 (2005).
7. Piccart-Gebhart, M.J. *et al.* Trastuzumab after adjuvant chemotherapy in HER2-positive breast cancer. *N. Engl. J. Med.* **353**, 1659–1672 (2005).
8. Yuan, Z.M. *et al.* Regulation of DNA damage-induced apoptosis by the c-Abl tyrosine kinase. *Proc. Natl. Acad. Sci. USA* **94**, 1437–1440 (1997).
9. Yoshida, K., Yamaguchi, T., Natsume, T., Kufe, D. & Miki, Y. JNK phosphorylation of 14–3-3 proteins regulates nuclear targeting of c-Abl in the apoptotic response to DNA damage. *Nat. Cell Biol.* **7**, 278–285 (2005).
10. Van Etten, R.A. Cycling, stressed-out and nervous: cellular functions of c-Abl. *Trends Cell Biol.* **9**, 179–186 (1999).
11. Sun, X. *et al.* Activation of the cytoplasmic c-Abl tyrosine kinase by reactive oxygen species. *J. Biol. Chem.* **275**, 17237–17240 (2000).
12. Li, B. *et al.* Distinct roles of c-Abl and Atm in oxidative stress response are mediated by protein kinase Cδ. *Genes Dev.* **18**, 1824–1837 (2004).
13. Deng, X. *et al. Caenorhabditis elegans* ABL-1 antagonizes p53-mediated germline apoptosis after ionizing irradiation. *Nat. Genet.* **36**, 906–912 (2004).
14. Cao, C., Leng, Y. & Kufe, D. Catalase activity is regulated by c-Abl and Arg in the oxidative stress response. *J. Biol. Chem.* **278**, 29667–29675 (2003).
15. Cao, C., Leng, Y., Huang, W., Liu, X. & Kufe, D. Glutathione peroxidase 1 is regulated by the c-Abl and Arg tyrosine kinases. *J. Biol. Chem.* **278**, 39609–39614 (2003).
16. Vasan, R.S., Levy, D., Larson, M.G. & Benjamin, E.J. Interpretation of echocardiographic measurements: a call for standardization. *Am. Heart J.* **139**, 412–422 (2000).
17. Khan, M.A. Effects of myotoxins on skeletal muscle fibers. *Prog. Neurobiol.* **46**, 541–560 (1995).
18. Daniels, C.E. *et al.* Imatinib mesylate inhibits the profibrogenic activity of TGF-β and prevents bleomycin-mediated lung fibrosis. *J. Clin. Invest.* **114**, 1308–1316 (2004).
19. Schermuly, R.T. *et al.* Reversal of experimental pulmonary hypertension by PDGF inhibition. *J. Clin. Invest.* **115**, 2811–2821 (2005).
20. Wolff, N.C. & Ilaria, R.L., Jr. Establishment of a murine model for therapy-treated chronic myelogenous leukemia using the tyrosine kinase inhibitor STI571. *Blood* **98**, 2808–2816 (2001).
21. le Coutre, P. *et al. In vivo* eradication of human BCR/ABL-positive leukemia cells with an ABL kinase inhibitor. *J. Natl. Cancer Inst.* **91**, 163–168 (1999).
22. Hu, Y. *et al.* Requirement of Src kinases Lyn, Hck and Fgr for BCR-ABL1-induced B-lymphoblastic leukemia but not chronic myeloid leukemia. *Nat. Genet.* **36**, 453–461 (2004).
23. McLeod, C.J., Pagel, I. & Sack, M.N. The mitochondrial biogenesis regulatory program in cardiac adaptation to ischemia–a putative target for therapeutic intervention. *Trends Cardiovasc. Med.* **15**, 118–123 (2005).
24. Baines, C.P. *et al.* Loss of cyclophilin D reveals a critical role for mitochondrial permeability transition in cell death. *Nature* **434**, 658–662 (2005).
25. Sanbe, A. *et al.* Reversal of amyloid-induced heart disease in desmin-related cardiomyopathy. *Proc. Natl. Acad. Sci. USA* **102**, 13592–13597 (2005).
26. Yuan, J., Lipinski, M. & Degterev, A. Diversity in the mechanisms of neuronal cell death. *Neuron* **40**, 401–413 (2003).
27. Ankarcrona, M. *et al.* Glutamate-induced neuronal death: a succession of necrosis or apoptosis depending on mitochondrial function. *Neuron* **15**, 961–973 (1995).
28. Murriel, C.L., Churchill, E., Inagaki, K., Szweda, L.I. & Mochly-Rosen, D. Protein kinase Cδ activation induces apoptosis in response to cardiac ischemia and reperfusion damage: a mechanism involving BAD and the mitochondria. *J. Biol. Chem.* **279**, 47985–47991 (2004).
29. Steinberg, S.F. Distinctive activation mechanisms and functions for protein kinase Cδ. *Biochem. J.* **384**, 449–459 (2004).
30. Zhang, K. & Kaufman, R.J. Signaling the unfolded protein response from the endoplasmic reticulum. *J. Biol. Chem.* **279**, 25935–25938 (2004).
31. Boyce, M. *et al.* A selective inhibitor of eIF2α dephosphorylation protects cells from ER stress. *Science* **307**, 935–939 (2005).
32. Ron, D. Translational control in the endoplasmic reticulum stress response. *J. Clin. Invest.* **110**, 1383–1388 (2002).

33. Holcik, M. & Sonenberg, N. Translational control in stress and apoptosis. *Nat. Rev. Mol. Cell Biol.* **6**, 318–327 (2005).
34. Yoshida, H., Matsui, T., Yamamoto, A., Okada, T. & Mori, K. XBP1 mRNA is induced by ATF6 and spliced by IRE1 in response to ER stress to produce a highly active transcription factor. *Cell* **107**, 881–891 (2001).
35. Lee, A.H., Iwakoshi, N.N. & Glimcher, L.H. XBP-1 regulates a subset of endoplasmic reticulum resident chaperone genes in the unfolded protein response. *Mol. Cell. Biol.* **23**, 7448–7459 (2003).
36. Urano, F. *et al.* Coupling of stress in the ER to activation of JNK protein kinases by transmembrane protein kinase IRE1. *Science* **287**, 664–666 (2000).
37. Nishitoh, H. *et al.* ASK1 is essential for endoplasmic reticulum stress-induced neuronal cell death triggered by expanded polyglutamine repeats. *Genes Dev.* **16**, 1345–1355 (2002).
38. Borsello, T. *et al.* A peptide inhibitor of c-Jun N-terminal kinase protects against excitotoxicity and cerebral ischemia. *Nat. Med.* **9**, 1180–1186 (2003).
39. Baines, C.P. & Molkentin, J.D. STRESS signaling pathways that modulate cardiac myocyte apoptosis. *J. Mol. Cell. Cardiol.* **38**, 47–62 (2005).
40. Gorre, M.E. *et al.* Clinical resistance to STI-571 cancer therapy caused by BCR-ABL gene mutation or amplification. *Science* **293**, 876–880 (2001).
41. Pattacini, L. *et al.* Endoplasmic reticulum stress initiates apoptotic death induced by STI571 inhibition of p210 bcr-abl tyrosine kinase. *Leuk. Res.* **28**, 191–202 (2004).
42. Ito, Y. *et al.* Targeting of the c-Abl tyrosine kinase to mitochondria in endoplasmic reticulum stress-induced apoptosis. *Mol. Cell. Biol.* **21**, 6233–6242 (2001).
43. Rao, R.V., Ellerby, H.M. & Bredesen, D.E. Coupling endoplasmic reticulum stress to the cell death program. *Cell Death Differ.* **11**, 372–380 (2004).
44. Tournier, C. *et al.* Requirement of JNK for stress-induced activation of the cytochrome c-mediated death pathway. *Science* **288**, 870–874 (2000).
45. Aoki, H. *et al.* Direct activation of mitochondrial apoptosis machinery by c-Jun N-terminal kinase in adult cardiomyocytes. *J. Biol. Chem.* **277**, 10244–10250 (2002).
46. Tsuruta, F. *et al.* JNK promotes Bax translocation to mitochondria through phosphorylation of 14–3-3 proteins. *EMBO J.* **23**, 1889–1899 (2004).
47. Okada, M. *et al.* A novel mechanism for imatinib mesylate-induced cell death of BCR-ABL-positive human leukemic cells: caspase-independent, necrosis-like programmed cell death mediated by serine protease activity. *Blood* **103**, 2299–2307 (2004).
48. Schiller, N.B. *et al.* Recommendations for quantitation of the left ventricle by two-dimensional echocardiography. American Society of Echocardiography Committee on Standards, Subcommittee on Quantitation of Two-Dimensional Echocardiograms. *J. Am. Soc. Echocardiogr.* **2**, 358–367 (1989).
49. Haq, S. *et al.* Deletion of cytosolic phospholipase A2 promotes striated muscle growth. *Nat. Med.* **9**, 944–951 (2003).